Electrochimica Acta 55 (2010) 1239–1244

Contents lists available at ScienceDirect

Electrochimica Acta

journal homepage: www.elsevier.com/locate/electacta

Influence of sputtering power on oxygen reduction reaction activity of zirconium oxides prepared by radio frequency reactive sputtering

Yan Liu [a,*], Akimitsu Ishihara [b], Shigenori Mitsushima [b], Ken-ichiro Ota [b,1]

[a] Beijing National Laboratory for Molecular Sciences, State Key Lab for Structural Chemistry of Unstable and Stable Species, College of Chemistry and Molecular Engineering, Peking University, Beijing 100871, China
[b] Chemical Energy Laboratory, Yokohama National University, Yokohama 240-8501, Japan

ARTICLE INFO

Article history:
Received 21 April 2009
Received in revised form 15 October 2009
Accepted 19 October 2009
Available online 25 October 2009

Keywords:
Zirconium oxides
Non-platinum cathode
Radio frequency power
Oxygen reduction reaction
Polymer electrolyte fuel cells

ABSTRACT

Zirconium oxides (ZrO_{2-x}) have been investigated as new cathodes for direct methanol fuel cells without platinum. ZrO_{2-x} films were prepared using a radio frequency (RF) magnetron sputtering at RF powers from 75 to 175 W. The influence of the RF power on the catalytic activity for the oxygen reduction reaction (ORR) and properties of the ZrO_{2-x} films were examined. The ORR activity of the ZrO_{2-x} catalyst increased with the RF power in the range we studied. The onset potential for ORR over ZrO_{2-x} deposited at 175 W was 0.88 V vs RHE. In addition, the relationship between the ORR activity and the composition, crystallinity, electric conductivity, as well as the ionization potential has been investigated. The zirconium oxide with an oxygen defected state and the higher electric conductivity showed the higher ORR activity, and the electrocatalytic activity for ORR increased with the decreasing in the ionization potential of the ZrO_{2-x} catalyst.

1. Introduction

Cathode electrocatalysts with excellent oxygen reduction reaction (ORR) activity and excellent methanol tolerance properties are vital materials in developing high efficient direct methanol fuel cells (DMFCs) for the applications in transportation and portable electronic devices. Highly dispersed platinum on carbon powder has been widely used as an oxygen reduction electrocatalyst in DMFC systems. However, the methanol crossover in DMFCs equipped with such a cathode results in the competitive oxidation reaction of methanol over the cathode, which severely decreases the cell's performance and energy transformation efficiency [1]. Moreover, it is not easy to obtain the required efficiency even using platinum which has some limitations of its catalytic property for ORR [2,3]. Except that, platinum is expensive and resources are very limited. Considering the cost and resource of platinum, many attempts are going to reduce the Pt loading. However, because the dissolution of highly dispersed Pt particles became a serious problem for the long-time operation of the fuel cell system, it was becoming clear that the drastic reduction of Pt use was actually difficult. Therefore, the development of stable, methanol-tolerant and non-noble catalysts for ORR is strongly required to widely commercialize DMFC.

Various materials have been proposed as cost-effective, non-noble and methanol-tolerant cathodic catalysts for DMFC. Transition metal macrocyclic compounds (e.g., porphyrins, phthalocyanines, tetraazannulenes) showed remarkable selectivity to ORR and inertness to MOR [4–7]. However, they show low electrochemical (chemical) stability in acidic conditions. Some transition metal macrocycles after heat treatment have shown improved activity and stability for ORR [5,8]. Transition metal chalcogenides, such as, chevrel phase-type compounds (e.g., $Mo_{6-x}M_xX_8$) and amorphous phase compounds (e.g., $Ru_xMo_ySe_z$, Ru_xS_y) also have been investigated for use as methanol-tolerant ORR catalysts [9–11]. Ru-based chalcogenides displayed the best activity in acid conditions among other metals tested. However, it should point out that Ru-based chalcogenides may not be real non-noble catalysts because ruthenium is actually a noble metal, which is also very expensive. In addition, long-term chemical stability is probably an even more serious for this category of electrocatalysts. Transition metal oxides, especially those with a perovskite or pyrochlore structure that allows easy exchange of oxygen, showed remarkable activity for ORR in an alkaline solution. Unfortunately, most transition metal oxides have been found to be unstable in the acidic environment of PEM fuel cell operation [12]. We believe that a high stability is an essential requirement because the cathode catalysts are exposed to an acidic and oxidative atmosphere, that is, a strong corrosive environment. In our previous work, we found that the zirconium oxide (ZrO_{2-x}) prepared by RF reactive sputtering [13,14] and titanium oxide prepared by heat treatment of titanium sheets [15] were stable in an acid solution and had a definite catalytic activ-

* Corresponding author. Tel.: +86 10 62751491; fax: +86 10 62765769.
E-mail address: liu-yan@pku.edu.cn (Y. Liu).
[1] ISE member.

0013-4686/$ – see front matter © 2009 Elsevier Ltd. All rights reserved.
doi:10.1016/j.electacta.2009.10.042

ity for the ORR. Moreover, ZrO_{2-x} performed excellent methanol tolerance and high selectivity for ORR in the presence of methanol [14]. From rotating disk electrode (RDE) experiments, it was concluded by S.V. Mentus that the ORR on anodically formed TiO_2 on Ti surface proceeds through a two-electron process in acidic solutions and four-electron process in basic solutions [16]. However, the ORR activity of these transition metal oxides was not very high in acidic solutions, and the factor which affected the catalytic activity has not yet been clarified.

The physicochemical properties and microstructure of the sputtered films are strongly influenced by the deposition condition, such as RF power [17], substrate temperature [18], substrate–target distance[17], oxygen percentage[19,20] in the sputtering gases in the case of a RF reactive magnetron sputtering. Because the RF power during ZrO_{2-x} deposition was expected to affect the catalytic activity for ORR, in this study, ZrO_{2-x} thin films have been prepared by the RF reactive magnetron sputtering using different RF power. The RF power was changed from 75 to 175 W during the deposition, and the influence of the RF power on the ORR catalytic activity of ZrO_{2-x} in the presence of methanol was investigated. In addition, the effect of the RF power on the properties of ZrO_{2-x}, such as the chemical composition, the crystalline structure, the crystallinity, the ionization potential, and the electric conductivity was also examined and the correlation between the catalytic activity for the ORR and the properties was discussed.

2. Experimental

The zirconium oxide catalysts were sputtered on the end of a glassy carbon rod substrate (5.2 ⌀ × 10 mm length, Tokai Carbon) by a RF magnetron sputtering method using an MUE–ECO–EV apparatus (ULVAC). Prior to the sputtering, the surface of the glassy carbon (GC) was polished by lapping tape LT-2000, LT-4000 and LT-6000 (FuJi Film Co., Japan) by turns to a mirror finish. The zirconium oxide target (ZrO_2, 99.9% purity, Furuuchi Chemical Co., Japan), with a diameter of 50.7 mm, was used as cathode. The vacuum chamber was evacuated down to 10^{-3} Pa using a turbomolecular pump. The sputtering gas, Argon with a purity of 99.99% was controlled by a standard mass-flow controller. The sputtering pressure was 3.0×10^{-1} Pa. Before deposition, the target was cleaned by sputtering with a RF power of 50 W for 5 min, while the glassy carbon was covered with a shield. The substrate was heated by a halogen lamp heater during the sputtering. The RF power was changed from 75 to 175 W and fixed the substrate temperature at 500 °C. The distance between the target and the glassy carbon was ca. 24 cm. The film thickness was ca. 25 nm measured by a QCM film thickness meter.

The crystalline properties of the cross-section surface of the zirconium oxides were observed by Transmission Electron Microscope (TEM) (HITACHI H-9500) under an accelerating voltage of 300 kV. The sample of the thicknesses about 60 nm was prepared by Focused Ion Beam (FIB) techniques. The electron diffraction patterns of crystal obtained by Fast Fourier Transform (FFT) of the TEM images were used to determine the crystalline structure.

The surface composition of zirconium oxides was measured by XPS (X-ray photo-electron spectroscopy, JPS-9200, JEOL) measurements, and determined using Zr 3d and O 1 s spectra. The XPS measurements were performed by Al Kα (1486.6 eV) radiation after removed the contaminants at the film surface by Ar-sputtering. The binding energy scale was calibrated to Au $4f_{7/2}$ (84 eV). For charge referencing adventitious C 1 s peak at 284.8 eV was used. The ionization potential of zirconium oxides was measured by PESA (photo-electron spectroscopy in air, AC-2, Rikenkeiki, Japan). The electric conductivity of zirconium oxides was tested by four-terminal resistance measurement.

Table 1
Oxidation and reduction charge of glassy carbon (GC) and ZrO_{2-x}.

RF power/W	GC	75	100	125	150	175
Q_a/μC	11.3	16.1	26.5	29.2	34.6	32.6
Q_c/μC	11.8	15.8	27.8	28.7	34.4	31.6

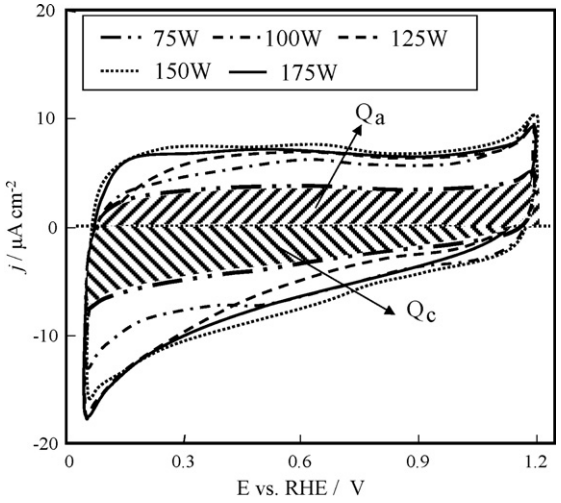

Fig. 1. CVs of ZrO_{2-x} deposited at different RF power under N_2 in 0.1 M H_2SO_4 at 30 °C Scan rate: 50 mV s^{-1}.

The electrochemical experiments were conducted in a three-electrode glass cell to do the following electrochemical measurements: (i) The electrochemical stability of the zirconium oxides were investigated by cyclic voltammetry (CV) in the potential range of 1.2–0.05 V with a scan rate of 50 mV s^{-1}; (ii) After the electrode reached a steady state, the ORR activity was measured by slow scan voltammetry (SSV) from 1.2 to 0.05 V (cathodic potential scan) with a scan rate of 5 mV s^{-1}. The electrolyte was a sulfuric acid (0.1 M) with or without methanol (0.1 M). The working electrode (the GC rod with the zirconium oxide film on its base) was connected with a potentiostat by a gold line. The side of the GC rod was coated with nail polish. The reference electrode was a reversible hydrogen electrode (RHE). All the potentials reported in the paper were expressed with respect to a RHE. The catalytic activity for ORR of all the catalysts was evaluated by the potential–current curve that was obtained from the difference of current density between the O_2 and N_2 atmospheres $i_{O_2-N_2} = i_{O_2} - i_{N_2}$ in the cathodic potential scan. The HZ3000 electrochemical measurement system (Hokuto Denko, Japan) was used in these measurements.

3. Results and discussion

3.1. Electrochemical stability

Fig. 1 shows the 10th cycle of the cyclic voltammograms (CVs) of ZrO_{2-x} film electrodes deposited at different RF power in 0.1 M sulfuric acid under a nitrogen atmosphere at 30 °C. The potential range was from 1.2 to 0.05 V with a scan rate of 50 mV s^{-1}. The current densities were expressed in terms of the geometric surface area of the electrodes. The CVs approached a steady state easily after 2 cycles. No specific oxidation or reduction current peaks were observed in the CVs. In addition, the oxidation and reduction charges at the steady state presented in the diagonal lines were calculated and summarized in Table 1. The oxidation charge was close to the reduction charge for all the samples. It indicated quantitatively that a one-sided redox reaction did not occur over these ZrO_{2-x} electrodes. They were stable in acid medium at least in the potential range for ORR.

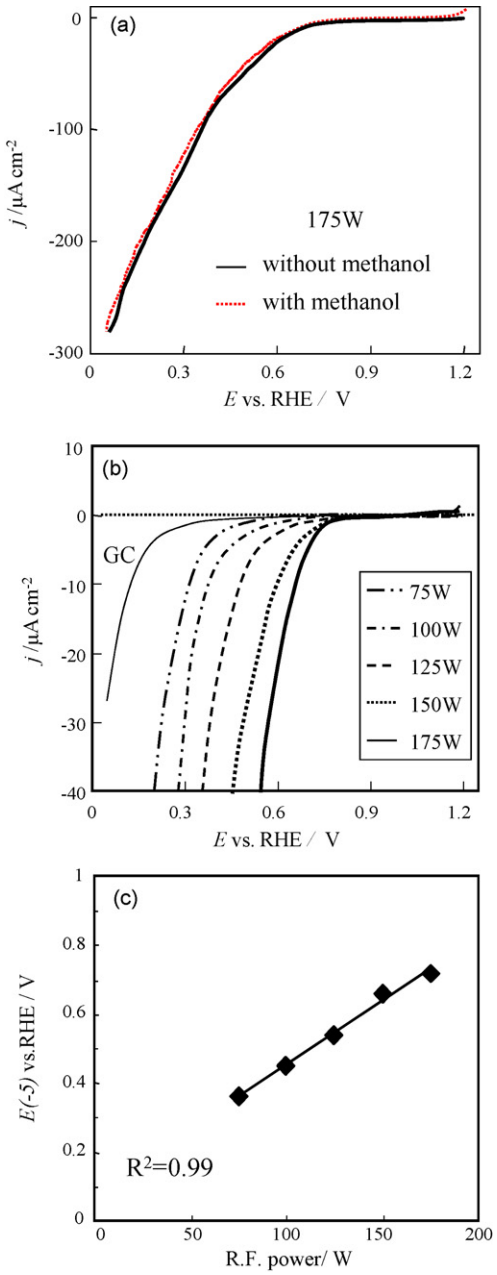

Fig. 2. a. Potential–current curves of ZrO_{2-x} deposited at 175 W in O_2-saturated 0.1M H_2SO_4 with or without 0.1 M methanol; b. potential–current curves of GC and ZrO_{2-x} deposited at different RF power in O_2-saturated 0.1M H_2SO_4 without methanol at 30 °C (scan rate: 5 mV s^{-1}); c. the variation of ORR activity over ZrO_{2-x} catalysts with the RF power.

3.2. Catalytic activity for ORR

Fig. 2a shows the potential–current curves over ZrO_{2-x} electrode deposited at 175 W in 0.1 M H_2SO_4 with or without 0.1 M methanol under an oxygen atmosphere. The potential was scanned from 1.2 to 0.05 V with a scan rate of 5 mV s^{-1}. The two curves for the ZrO_{2-x} electrode in the presence and in the absence of methanol almost overlapped. The same results were obtained over the ZrO_{2-x} electrode deposited at other RF powers. The mixed potential as found on Pt catalyst was not observed on the ZrO_{2-x} catalysts. Moreover, the limiting current which controls by the oxygen diffusion was not observed over the ZrO_{2-x} catalysts at the low potential region until 0.05 V.

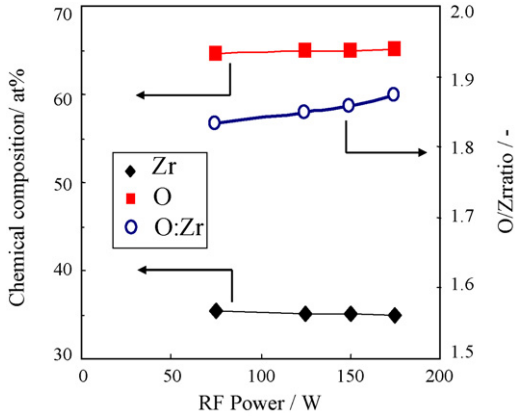

Fig. 3. The variation of the chemical composition of ZrO_{2-x} with the RF power.

Fig. 2b summarizes the potential–current curves over the GC and ZrO_{2-x} electrodes deposited at different RF power in O_2-saturated 0.1 M H_2SO_4 without methanol at 30 °C. In comparison with the GC, an apparent increase of the reduction current was observed over all these ZrO_{2-x} catalysts. The onset potential for ORR over ZrO_{2-x} deposited at 175 W was 0.88 V vs RHE, which was shifted positively by about 300 mV over ZrO_{2-x} deposited at 75 W. According to the results, ZrO_{2-x} deposited at higher RF power has a definite catalytic activity for ORR even in the presence of methanol.

The potential at the reduction current of -5 μA cm^{-2}, $E(-5)$, is used as an evaluation indicator for the ORR activity. Fig. 2c shows the relationship of $E(-5)$ over ZrO_{2-x} catalysts with the RF power. $E(-5)$ is proportionally to the RF power and increases significantly by increasing the RF power. This indicated that the ORR activity over ZrO_{2-x} catalysts increased with the RF power in the range we studied.

3.3. Characterization of ZrO_{2-x}

The chemical composition at the surface of ZrO_{2-x} film electrodes was determined using XPS analyses. Although the signal ratio of XPS could not be corresponded to an exact chemical composition, it could be possible to compare the relative content among the specimens. Fig. 3 shows the variation of chemical composition of ZrO_{2-x} with the RF power. The atomic percent of Zr and O was almost same among the specimens deposited at different RF power, and the O/Zr atomic ratio at the surface of ZrO_{2-x} was ca. 1.85 ± 0.02. It indicated that the surface of the ZrO_{2-x} catalysts was oxygen defected state and partially reduced. It should point out here that we have found that the zirconium oxide with a complete oxidation state (ZrO_2) is not active for ORR [21].

Fig. 4 shows the SEM images of ZrO_{2-x} catalysts. Clear crystal grains can be observed in all the specimens. It indicated that the major part of ZrO_{2-x} prepared with different RF power at 500 °C should be crystal. No obvious difference in surface morphologies and particles size were observed in the ZrO_{2-x} deposited at different RF power. The average size of crystal grains was 20–30 nm.

Fig. 5a–c shows the cross-sectional TEM images of the ZrO_{2-x} deposited at different RF power. Each ZrO_{2-x} film was uniformly formed, and the thickness was estimated to be approximately 25 nm. According to the interface between the ZrO_{2-x} film and the glassy carbon as shown in Fig. 5c, we believed that the adhesion between the ZrO_{2-x} film and the glassy carbon support was strong enough. Crystal lattice areas were observed in all of the specimens. The electron beam diffraction patterns of the crystal lattice were obtained using a Fourier transform mapping of the TEM images. Fig. 5d–h shows the electron beam diffraction patterns of the ZrO_{2-x} film. The electron diffraction pattern of the ZrO_{2-x} deposited at

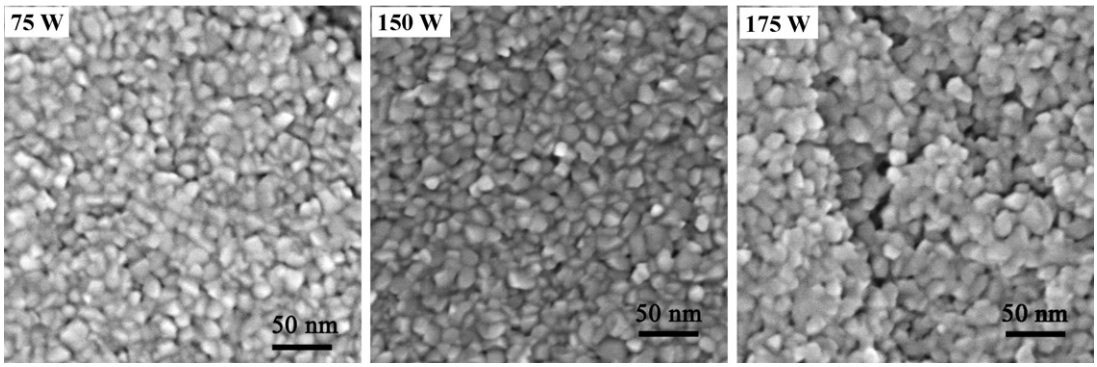

Fig. 4. SEM images of ZrO_{2-x} catalysts deposited at different RF power.

75 W in Fig. 5d shows well-defined (1 0 1) lattice fringes with 2.98, 2.61, and 3.20 Å spacing, indicating that the film consists of monoclinic crystalline structure of ZrO_2 (JCPDS 37-1484). Fig. 5e shows (110) lattice fringes with 2.62, 2.99, and 3.03 Å spacing, indicating that the film consists of hexagonal crystalline structure of ZrO_2 (JCPDS 37-31), too. The same as the ZrO_{2-x} deposited at 75 W, the monoclinic and hexagonal crystalline structures were observed also in the ZrO_{2-x} deposited at 150 W (f, g) and 175 W (h). This provides proof that the ZrO_{2-x} films deposited at different RF power consist of poly-phase crystals.

The uniform crystal lattice fringes could be observed in most of the particles through the TEM images. In order to evaluate the crystal growth at different RF power, the crystallinity was defined as the following equation:

$$\text{Crystallinity} = \frac{\sum_{i=1}^{n} \text{Area}_{\text{cryst.}}}{\text{Area}_{\text{total}}}$$

As shown in Fig. 6a, $\text{Area}_{\text{total}}$, the total area of the particles is calculated from the part surrounded by a break line. $\text{Area}_{\text{cryst.}}$, the crystalline area is calculated from each crystal lattice fringe part, for example as the part surrounded by a solid line. Fig. 6b shows the variation of crystallinity of ZrO_{2-x} with the RF power. The crys-

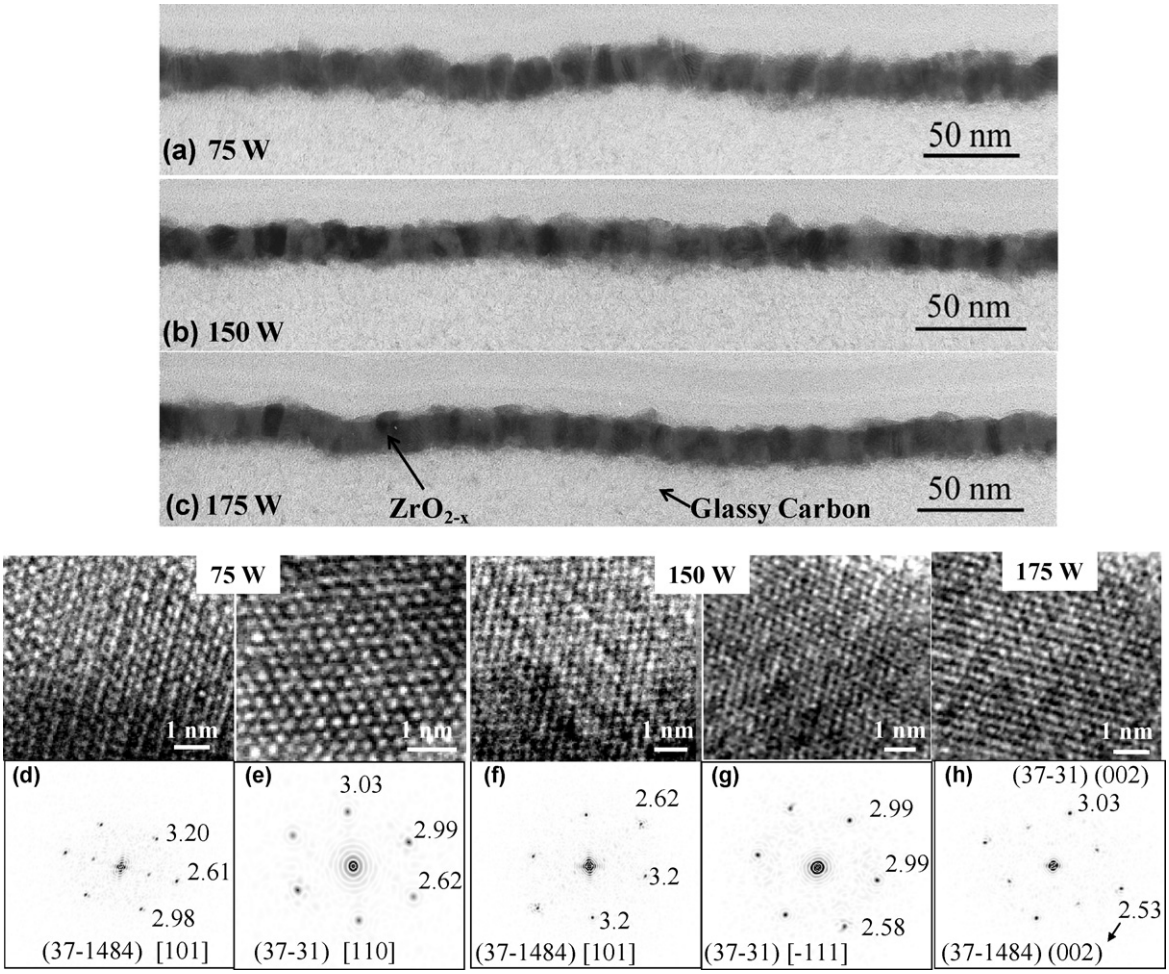

Fig. 5. Cross-sectional surface of TEM images (a–c) and electron diffraction patterns of ZrO_{2-x} deposited at 75 W (d–e), 150 W (f–g), and 175 W (h).

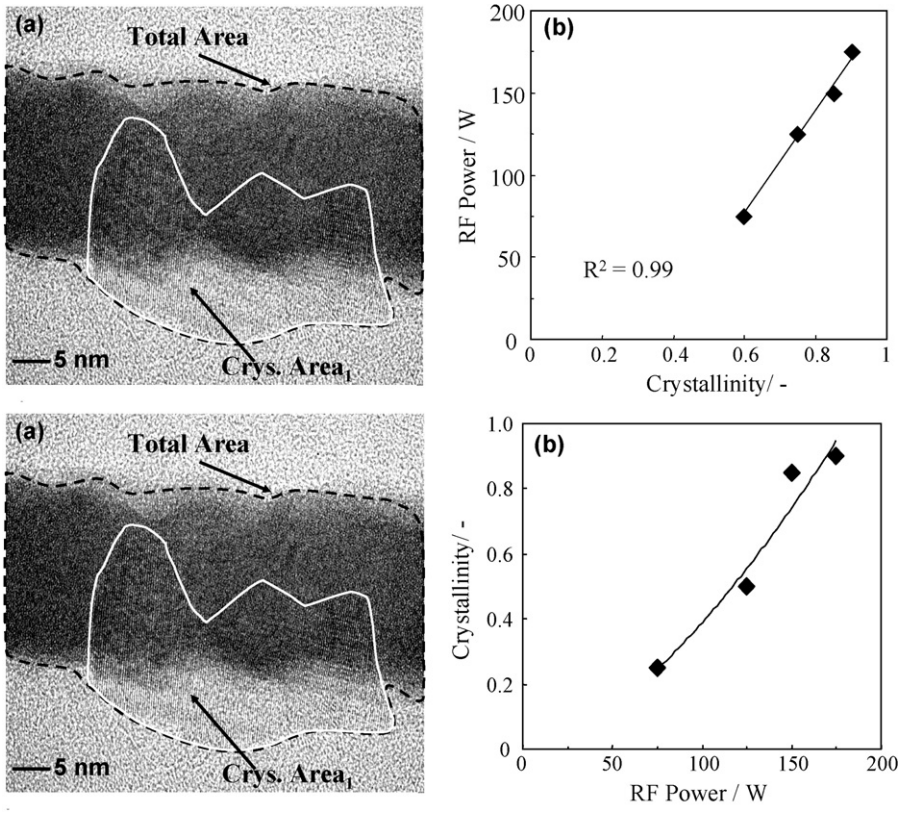

Fig. 6. a. Schematic representation for calculating the crystallinity from TEM image; b. the variation of the crystallinity of ZrO_{2-x} with the RF power.

tallinity was about 60%, 75%, 85% and 90% for the ZrO_{2-x} deposited at 75 W, 125 W, 150 W and 175 W, respectively. The crystallinity is proportional to the RF power and increases with the increasing of the RF power. These results indicated that the ZrO_{2-x} prepared using reactive sputtering was easy to crystallize by controlling the applied RF power at a relative low temperature.

3.4. Relationship between ORR activity and properties of ZrO_{2-x}

Fig. 7 shows the relationship between ORR activity with the crystallinity over ZrO_{2-x} catalyst. $E(-5)$ increased with the increase of the crystallinity, namely, the electrocatalytic activity for the ORR over ZrO_{2-x} catalyst increased with the crystallinity. We believed that crystallinity played a significant role in the ORR. It was still not clear for the mechanism between ORR activity and crystallinity. It was considered that the ZrO_{2-x} with a high crystallinity might improve the surface adsorption of the oxygen and lead to the increase in the ORR kinetics for the ZrO_{2-x} catalyst.

The adsorption of oxygen molecules on the surface is required as the first step in the ORR process. The quantity of the adsorbed oxygen on the electrode surface is an important factor in the kinetics of the oxygen reduction. Knowledge of the detailed surface electronic structure is critical in the understanding of the chemisorptive and catalytic properties. The ionization potential is one of the important electronic parameters of the metal oxides. The measurements of conductivity of oxides have been a source of knowledge about the mechanism of oxygen adsorption.

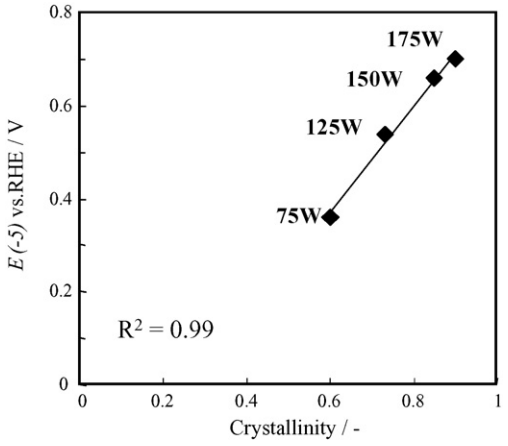

Fig. 7. Relationship between ORR activity over ZrO_{2-x} catalyst with the crystallinity.

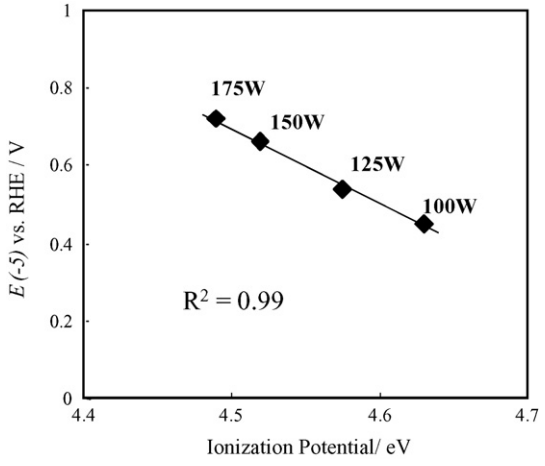

Fig. 8. Relationship between ORR activity over ZrO_{2-x} catalyst with the ionization potential.

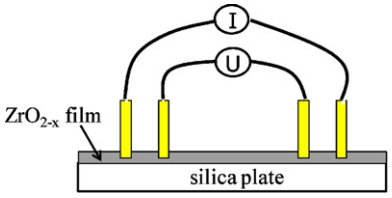

Sample	Resistivity(Ω□cm)	O/Zr ratio*
75 W	6×10^5	1.83
150 W	9×10^4	1.85
175 W	5×10^4	1.87

Fig. 9. Electric conductivity of zirconium oxide film (ca. 200 nm) sputtered at different RF power on a silica plate. (*) O/Zr ratio derived from Fig. 3.

Fig. 8 shows the relationship between ORR activity over ZrO_{2-x} catalyst with the ionization potential. The ionization potential decreased with the increase in the RF power, and the ORR activity increased with the decreasing of the ionization potential. It has been reported by Enikeev, et al. that the activation energy of the oxygen adsorption increases with the ionization potential on the metal oxides, such as ZnO oxide [22]. The ZrO_{2-x} with a low ionization potential would be expected to allow a facile oxygen adsorption on the electrode surface, corresponding to an increase in the concentration of the reactive oxygen.

As shown in Fig. 9, the electric conductivity of zirconium oxide film (thickness: ca. 200 nm) sputtered at different RF power on a silica plate was tested by four-terminal resistance measurement. The resistivity decreased with the increase in the RF power. The results in Fig. 3 have shown that the zirconium oxides deposited at RF power from 75 to 175 W are an oxygen defected state. That is to say, these zirconium oxides are N-type semiconductor. Generally, the conductivity of N-type semiconductor oxides increases with an increase in the pressure of oxygen [23]. It has been revealed that the presence of surface defects sites is required to adsorb the oxygen molecules on the surface of the oxides such as $Ce_xZr_{(1-x)}O_2$, TiO_2 (1 1 0), V_2O_5, and MoO_3 [24–26]. Therefore, the surface defects on the ZrO_{2-x} affected the adsorption sites of oxygen molecules and could yield the increase in the electric conductivity. According to our results, the zirconium oxide with an oxygen defected state and the higher electric conductivity showed the higher ORR activity. The zirconium oxide with a high conductivity might obtain a high coverage of the adsorbed oxygen. This would lead to the increase in the ORR kinetics, in other words, the electrocatalytic activity for the ORR increased.

The variation of the crystallinity might also affect the electronic parameters of the electocatalysts and change the chemisorptive and catalytic properties of the metal oxides. A further investigation is required to clarify the effect of the crystallinity, the electric conductivity, as well as the surface defects of the ZrO_{2-x} on the catalytic activity for the ORR.

4. Conclusions

In order to improve the electrocatalytic activity of zirconium oxides for the ORR, the influence of the RF power on the ORR activity of the ZrO_{2-x} was investigated in sulfuric acid. The ORR activity over ZrO_{2-x} catalysts increased with the RF power in the range we studied. The onset potential for ORR over ZrO_{2-x} deposited at 175 W, was 0.88 V vs RHE, which was shifted positively by about 300 mV over ZrO_{2-x} deposited at 75 W. In addition, the zirconium oxide with an oxygen defected state and the higher electric conductivity showed the higher ORR activity, and the electrocatalytic activity for ORR increased with the decreasing in the ionization potential of the ZrO_{2-x} catalyst. In the presence of methanol, catalytic activity of ZrO_{2-x} toward ORR was not reduced.

Acknowledgments

The authors acknowledge the financial support received from the New Energy and Industrial and Technology Development Organization (NEDO, Japan), National Natural Science Foundation of China (NSFC, grants 20803001, 50821061) and RFDP 200800011012. The authors also acknowledge the apparatus support for the ionization potential measurement received from Rikenkeiki Co. JAP.

References

[1] M.H. Shao, K. Sasaki, R.R. Adzic, J. Am. Chem. Soc. 128 (2006) 3526.
[2] F.A. Uribe, M.S. Wilson, T.E. Springer, S. Gottesfeld, in: D.D Scherson, D. Tryk, M. Daroux, X. Xing (Eds.), Structural Effects in Electrocatalysis and Oxygen Electrochemistry, Proc. vol. 92-11, The Electrochem. Soc. Inc., Pennington, 1992, p. 494.
[3] D.M. Bernardi, M.W. Verbrugge, J. Electrochem. Soc. 139 (1992) 2477.
[4] R. Jasinski, Nature 201 (1964) 1212.
[5] R.Z. Jiang, D. Chu, J. Electrochem. Soc. 147 (2000) 4605.
[6] S. Baranton, C. Coutanceau, C. Roux, F. Hahn, J.M. Leger, J. Electroanal. Chem. 577 (2005) 223.
[7] H.S. Liu, C.J. Song, Y.H. Tang, J.L. Zhang, J.J. Zhang, Electrochim. Acta 52 (2007) 4532.
[8] G.Q. Sun, J.T. Wang, R.F. Savinell, J. Appl. Electrochem. 28 (1998) 1087.
[9] N. Alonso-Vante, P. Bogdanoff, H. Tributsch, J. Catal. 190 (2000) 240.
[10] T.J. Schmidt, U.A. Paulus, H.A. Gasteiger, N. AlonsoVante, R.J. Behm, J. Electrochem. Soc. 147 (2000) 2620.
[11] O. Solorza-Feria, K. Ellmer, M. Giersig, N. Alonso-Vante, Electrochim. Acta 39 (1994) 1647.
[12] R.W. Reeve, P.A. Christensen, A.J. Dickinson, A. Hamnett, K. Scott, Electrochim. Acta 45 (2000) 4237.
[13] Yan Liu, A. Ishihara, S. Mitsushima, N. Kamiya, K. Ota, J. Electrochem. Soc. 154 (2007) B664.
[14] Yan Liu, A. Ishihara, S. Mitsushima, N. Kamiya, K. Ota, Electrochem. Solid-State Lett. 8 (2005) A400.
[15] J.H. Kim, A. Ishihara, S. Mitsushima, N. Kamiya, K. Ota, Electrochim. Acta 52 (2007) 2492.
[16] S.V. Mentus, Electrochim. Acta 50 (2004) 27.
[17] P.T. Gao, L.J. Meng, M.P. dos Santo, V. Teixeira, M. Andritschky, Thin Solid Films 377 (2000) 557.
[18] S. Ben Amor, B. Rogier, G. Baud, M. Jacqueta, M. Nardin, Mater. Sci. Eng. B57 (1998) 28.
[19] P.T. Gao, L.J. Mengb, M.P. dos Santo, V. Teixeira, M. Andritschky, Appl. Surf. Sci. 173 (2001) 84.
[20] P.T. Gao, L.J. Meng, M.P. dos Santo, V. Teixeira, M. Andritschky, Vacuum 56 (2000) 143.
[21] K. Ota, N. Kamiya, S. Mitsushima, A. Ishihara, Yan Liu, Patent No. JAP 2005-364627.
[22] E.Kh. Enikeev, L.Ya. Margolis, S.Z. Rogonskii, Dokl. Akad. Nauk. SSSR 130 (1960) 807.
[23] V.F. Kiselev, O.V. Krylov (Eds.), Adsorption and Catalysis on Transition Metals and Their Oxides, Chapter 4, Springer-Verlag, Berlin Heidelberg New York, 1989, p. 177.
[24] A.L. Lisebigler, G. Lu, J.T. Yates Jr., Chem. Rev. (Washington, DC) 95 (1995) 735.
[25] C. Descorme, Y. Madier, D. Duprez, J. Catal. 196 (2000) 167.
[26] M. Witko, R. Tokarz-Sobieraj, Catal. Today 91–92 (2004) 171.